

Stable Solution-Processed High-Mobility Substituted Pentacene Semiconductors

Yuning Li, Yiliang Wu, Ping Liu, Zorica Prostran, Sandra Gardner, and Beng S. Ong*

New Materials Design and Synthesis Lab, Xerox Research Centre of Canada,
Mississauga, Ontario, Canada L5K 2L1

Received October 5, 2006. Revised Manuscript Received November 17, 2006

The synthesis, photooxidative stability, and field-effect transistor properties of a series of 6,13-diethynyl-substituted pentacene derivatives are described. Substitution with appropriate solubilizing ethynyl functions at the C-6/C-13 positions of pentacene, which promote extended π -electron delocalization from the pentacene nucleus, leads to phenomenal enhancement in both solubility and photooxidative stability. This has enabled fabrication of a stable, solution-processed thin-film semiconductor under ambient conditions for high-mobility organic thin-film transistors. Specifically, a solution-processed 6,13-bis(4-pentylphenylethynyl)pentacene semiconductor has yielded mobility as high as $0.52 \text{ cm}^2 \text{ V}^{-1} \text{ s}^{-1}$ in OTFTs.

Introduction

Pentacene is one of the most studied organic semiconductors for organic thin-film transistors (OTFTs),^{1–2} manifesting to the highest field-effect transistor (FET) mobility^{2c} among organic thin-film semiconductors. However, a pentacene thin-film semiconductor cannot be prepared using common solution deposition techniques due to its limited solubility, and its fabrication thus requires high vacuum evaporation. Most soluble substituted pentacene derivatives, on the other hand, are highly susceptible to photooxidation in solution (half-life: \sim few minutes),³ practically precluding their solution fabrication as functional thin-film semiconductors under ambient conditions. One effective approach to overcoming the photooxidation complication is via soluble pentacene precursors. Specifically, soluble cycloadducts bridged at the C-6 and C-13 positions of pentacene with cyclohexanediene⁴ and *N*-sulfinylamide⁵ have been successfully utilized in fabricating solution-processed thin-film semiconductors for OTFTs. Nonetheless, the thermal retro-conversion of these cycloadducts back to a high-mobility pentacene semiconductor necessitates high-temperature treatments, often requiring simultaneous protection from atmospheric oxygen.

The C-6/C-13 positions of pentacene are extremely sensitive to oxygen in solution when exposed to visible light in air.^{3b,6a,b} Recent efforts toward suppressing the photooxidative sensitivity of pentacene through judicious substitution have met with some success. In this respect, substitution of a bulky trialkylsilylethynyl such as triisopropylsilylethynyl (TIPS) at the C-6/C-13 positions of pentacene as in 6,13-bis(triisopropylsilylethynyl)pentacene (TIPS-pentacene) has proven to be effective for stabilization.⁷ Thus, a solution-processed TIPS-pentacene semiconductor was recently reported to give a mobility of $0.17 \text{ cm}^2 \text{ V}^{-1} \text{ s}^{-1}$ in OTFTs.^{7c} In our studies, we found that the photooxidative stability of the pentacene structure could be achieved through effective extended $-\pi$ -electron delocalization from the pentacene nucleus at the C-6/C-13 positions without the use of bulky trialkylsilyl groups. We report here our results on the synthesis of a new series of 6,13-diethynyl-substituted pentacenes, their photooxidative stability, and FET properties as solution-processed semiconductors in OTFTs. Mobility as high as $0.52 \text{ cm}^2 \text{ V}^{-1} \text{ s}^{-1}$ was obtained with an appropriately substituted pentacene, namely, 6,13-bis(4-pentylphenylethynyl)pentacene.

Results and Discussion

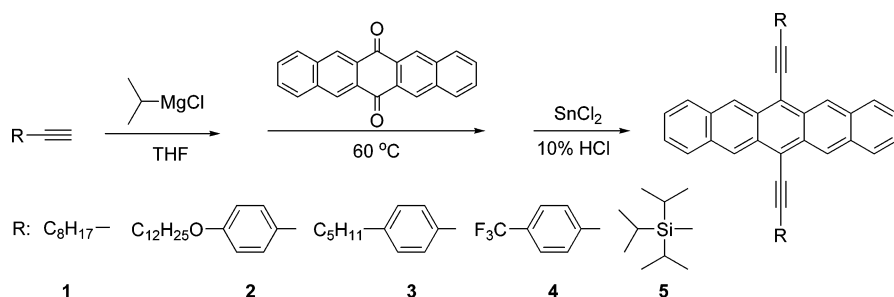
The synthesis of 6,13-diethynyl-substituted pentacenes is presented in Scheme 1. Substituted pentacene derivatives with 1-decynyl (**1**), 4-decyloxyphenylethynyl (**2**), 4-pentylphenylethynyl (**3**), and 4-trifluoromethylphenylethynyl (**4**) were readily synthesized from 6,13-pentacenequinone by reacting with the corresponding ethynylmagnesium chloride, followed by reduction with SnCl_2 . These substituted deriva-

* Corresponding author. E-mail: Beng.Ong@xrc.xerox.com.

- (1) (a) Dimitrakopoulos, C. D.; Mascaro, D. J. *Adv. Mater.* **2002**, *14*, 99–117. (b) Katz, H.; Bao, Z.; Gilat, S. *Acc. Chem. Res.* **2001**, *34*, 359–369.
- (2) Dimitrakopoulos, C. D.; Brown, A. R.; Pomp, A. *J. Appl. Phys.* **1996**, *80*, 2501–2508. (b) Lin, Y. Y.; Gundlach, D. J.; Nelson, S.; Jackson, T. N. *IEEE Trans. Electron Devices* **1997**, *44*, 1325–1331. (c) Kelly, T. W.; Boardman, L. D.; Dunbar, T. D.; Muires, D. V.; Pellerite, M. J.; Smith, T. P. *J. Phys. Chem. B* **2003**, *107*, 5877–5881.
- (3) (a) Allen, C. F.; Bell, A. *J. Am. Chem. Soc.* **1942**, *64*, 1253–1260. (b) Wolak, M. A.; Jang, B. B.; Palilis, L. C.; Kafafi, Z. H. *J. Phys. Chem. B* **2004**, *108*, 5492–5499.
- (4) (a) Brown, A. R.; Pomp, A.; Hart, C. M.; de Leew, D. M. *Science* **1995**, *270*, 972–974. (b) Brown, A. R.; Pomp, A.; de Leew, D. M.; Klassen, D. B. M.; Havinga, E. E.; Hertig, P. T.; Müllen, K. *J. Appl. Phys.* **1996**, *79*, 2136–2138. (c) Hertig, P. T.; Müllen, K. *Adv. Mater.* **1999**, *11*, 480–483.
- (5) (a) Afzali, A.; Dimitrakopoulos, C. D.; Breen, T. L. *J. Am. Chem. Soc.* **2002**, *124*, 8812–8813. (b) Weidkamp, K. P.; Afzali, A.; Tromp, R. M.; Hamers, R. J. *J. Am. Chem. Soc.* **2004**, *126*, 12740–12741.

- (6) (a) Maliakal, A.; Raghavachari, K.; Katz, H.; Chandross, E.; Siegrist, T. *Chem. Mater.* **2004**, *16*, 4980–4986. (b) Clar, E. *Polycyclic Aromatic Hydrocarbons*; Academic Press: London, 1964; Vol. 1.
- (7) (a) Anthony, J. E.; Brooks, J. S.; Eaton, D. L.; Parkin, S. R. *J. Am. Chem. Soc.* **2001**, *123*, 9482–9483. (b) Sheraw, C. D.; Jackson, T. N.; Eaton, D. L.; Anthony, J. E. *Adv. Mater.* **2003**, *15*, 2009–2011. (c) Payne, M. M.; Parkin, S. R.; Anthony, J. E.; Kuo, C. C.; Jackson, T. N. *J. Am. Chem. Soc.* **2005**, *127*, 4986–4987.

Scheme 1. Synthesis of 6,13-Diethynyl-Substituted Pentacenes



tives were obtained in fair to excellent overall yields (50–90%).

The UV–vis absorption spectra of 6,13-diethynyl-substituted pentacene derivatives in toluene solutions showed significant red shifts with λ_{\max} at 634, 664, 660, and 662 nm, respectively, for **1**–**4** as compared to parent pentacene ($\lambda_{\max} = 577$ nm) (Figure 1). This is indicative of an extended π -electron delocalization from the pentacene nucleus brought about by 6,13-diethynyl substitution. The fact that arylethynyl-substituted pentacenes **2**–**4** exhibited significantly larger red-shifts than TIPS-pentacene, **5** ($\lambda_{\max} = 643$ nm),⁷ showed that aryl function provided a more effective extended π -delocalization to the pentacene nucleus than TIPS.

The photooxidative stability of pentacene and its derivatives was studied by monitoring the reduction in absorbance at λ_{\max} in an air-saturated toluene solution under white light (fluorescent lamp) exposure at room temperature. Under these conditions, pentacene displayed a very short half-life time ($t_{1/2}$) of ~ 3 min, while all ethynyl-substituted pentacene derivatives exhibited significantly longer half-life times (Figure 2). Compound **4**, which has a bis(trifluorophenylethynyl) substitution, possessed the highest stability ($t_{1/2}$ of 9320 min), while compound **1**, which has a dialkylethynyl substitution, showed the lowest stability ($t_{1/2}$ of ~ 540 min) in this series. The observed stability order: **4** > **2** \approx **3** \gg **1** is in line with the expectation based on the effectiveness of respective ethynyl functions in providing extended π -electron delocalization via resonance/inductive effects. The earlier reported TIPS-pentacene **5** showed $t_{1/2}$ of 2700 min under our measuring conditions, which is about the same as those of **2** and **3**. These results clearly suggest that it was the electronic,^{6a} both resonance and inductive, and not the steric

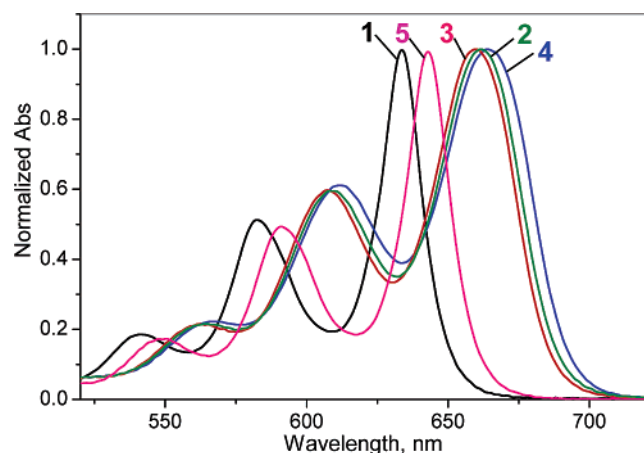


Figure 1. UV–vis spectra of 6,13-diethynyl-substituted pentacenes in toluene solution.

effect that was responsible for the stabilization of the pentacene nucleus in these cases. In other words, the bulky trialkylsilyl function is not mandatory, but rather it is the π -electron delocalization and withdrawal from the pentacene nucleus that are paramount. In addition, the bis(phenylethynyl)-substituted derivatives **2**–**4** exhibited excellent stability in the solid state when kept in the dark under ambient conditions (> 1 year), while didecynyl-substituted pentacene **1** showed complete structural degradation within a few months, presumably due to an intermolecular Diels–Alder reaction of ethynyl groups and the pentacene nucleus.⁸ The thermal stability of these substituted pentacenes also falls in the same order: **4** > **3** > **2** \gg **1**, with their decomposition temperatures at 243, 191, 162, and 109 °C, respectively. The decomposition of these substituted pentacenes was likely due to thermal polymerization of ethynyl groups or a Diels–Alder reaction during heating since large, sharp exothermic peaks were observed in their differential scanning calorimeter (DSC) profiles during heating scans. The higher thermal stability of arylethynyl-substituted pentacenes **4**, **3**, and **2** as compared to alkylethynyl-substituted pentacene **1** is a reflection of the relative stabilization of ethynyl function by the respective arylene moieties against polymerization or Diels–Alder reactions.

Both **2** and **4** were soluble in a variety of solvents (e.g., toluene, chlorobenzene, and dichlorobenzene) at elevated temperatures, but good quality films were difficult to obtain by solution techniques (e.g., spin-coating) due to their propensity to form crystal islands. On the other hand, **1** and

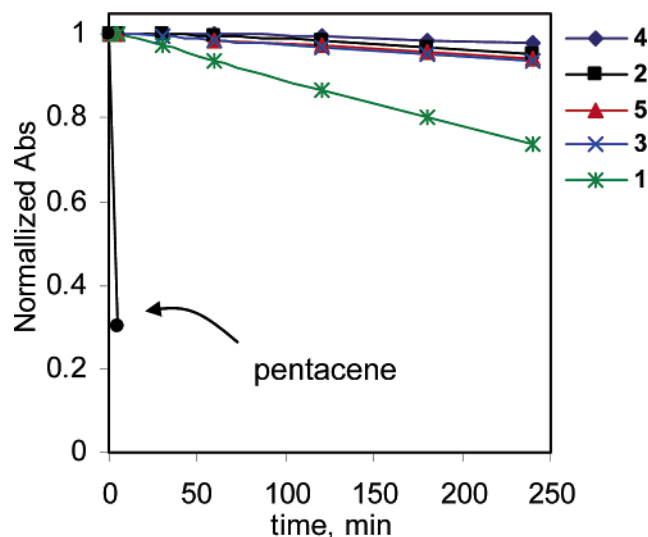


Figure 2. Normalized absorbance of pentacenes at λ_{\max} in toluene solution as a function of time under white light exposure in air.

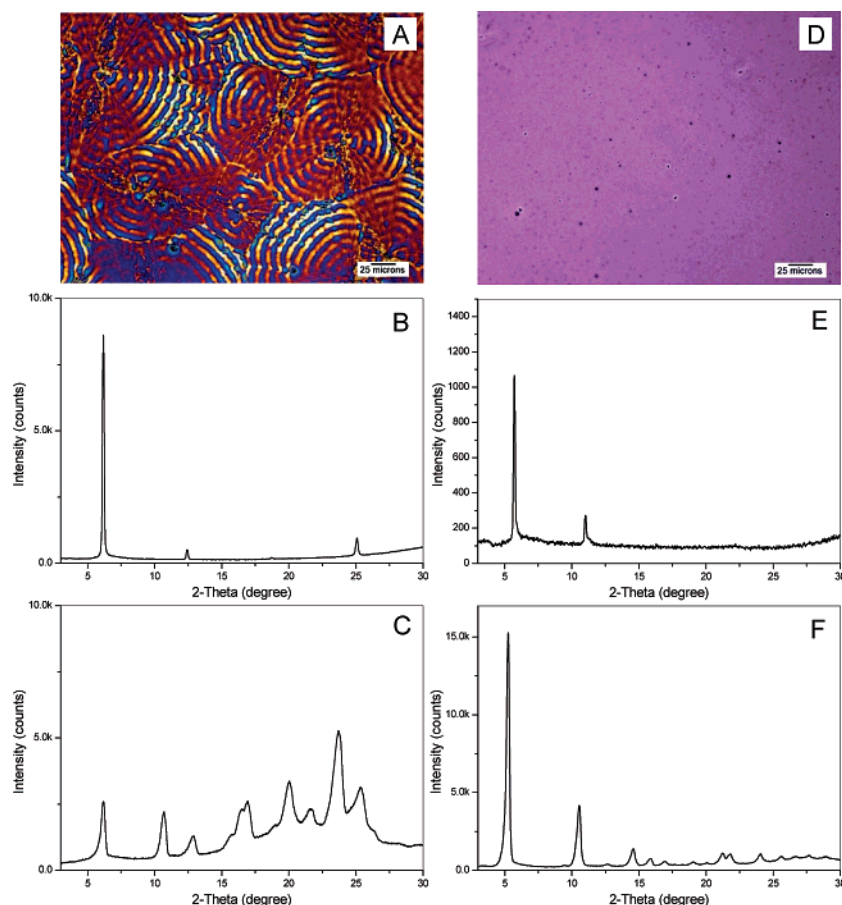


Figure 3. (A) Microscopic image of **1** (20 \times magnification); (B) XRD of spin-coated thin film of **1**; (C) powder XRD of **1**; (D) microscopic image of **3** (50 \times magnification); (E) XRD of spin-coated thin film of **3**; and (F) powder XRD of **3**.

3 readily formed continuous thin films when spin-coated from dilute solutions in chlorobenzene and 1,2-dichlorobenzene. Microscopic examination of a spin-cast thin film of **1** showed that it was crystalline with overlapping multiple concentric ringed structures having diameters of ~ 50 – 100 μm , indicating the formation of highly crystalline spherulites. The XRD pattern (Figure 3B) of this spin-cast film showed an intense, sharp primary diffraction peak at $2\theta = 6.18^\circ$, together with clearly defined second order to fourth order diffractions. However, powder XRD of **1** showed a far more complex diffraction pattern (Figure 3C), suggesting a more oriented molecular ordering of **1** in the spin-cast film. Similarly, the thin-film XRD pattern (Figure 3E) of **3** was simpler than its powder counterpart (Figure 3F), manifesting again a more oriented crystalline structure. Unlike **1**, **3** formed uniform spin-cast thin films showing no visible crystalline spherulite structures when viewed under a microscope.

We examined the single-crystal X-ray diffraction (XRD) of **3** closely since this molecule was of great interest from the perspectives of stability and FET properties. The XRD results revealed a closely packed layered structure with intimate π – π overlapping (Figure 4). Each of the π -stacks interweaved with one another in a herringbone manner at an angle of 82° . The interlayer distance is estimated to be

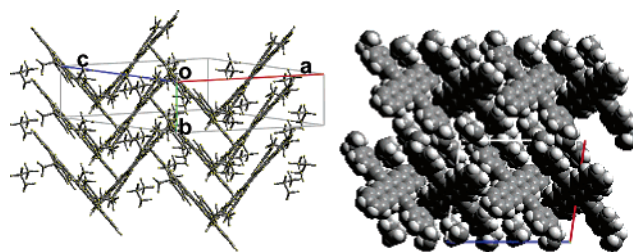


Figure 4. Single-crystal structures of compound **3** as viewed along the *ac*-layer (left) and *b*-axis (right).

3.44 \AA , an intermolecular distance that is favorable for charge carrier transport by intermolecular hopping. This molecular organization is slightly different from the herringbone structure of pentacene, which has a much smaller angle of 53° between two interweaving layers⁹ and completely different from the parallel layered structure of trialkylsilyl-ethynyl-substituted pentacene (e.g., TIPS-pentacene).^{7a}

6,13-Diethynyl-substituted pentacenes were evaluated as solution-deposited channel semiconductors in OTFTs using a bottom-gate, top-contact device configuration (Figure 5, inset). The device fabrication and characterization were carried out under ambient conditions. Specifically, the devices were built on an *n*-doped silicon wafer that served as the gate electrode, while its top thermal oxide layer (100 nm SiO_2) was the gate dielectric. The semiconductor was

(8) (a) Coppo, P.; Yeates, S. G. *Adv. Mater.* **2005**, *17*, 3001–3005. (b) Payne, M. M.; Odom, S. A.; Parkin, S. R.; Anthony, J. E. *Org. Lett.* **2004**, *6*, 3325–3328.

(9) Cornil, J.; Calbert, J. P.; Brédas, J. L. *J. Am. Chem. Soc.* **2001**, *123*, 1250–1251.

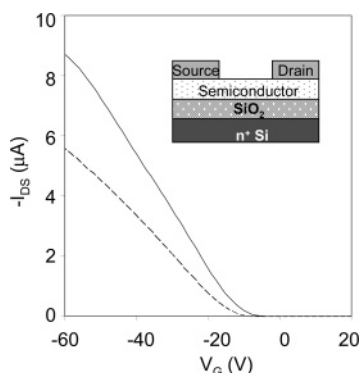


Figure 5. Transfer curves of illustrative OTFTs with 6,13-bis(4-pentylphenylethynyl)pentacene **3** as semiconductor deposited by spin-coating (dashed line) and dip-coating (solid line).

deposited from a dilute chlorobenzene solution by spin-coating, dip-coating, or drop-casting and dried in vacuo. Thereafter, the gold source/drain electrode pairs were vacuum deposited through a shadow mask, thus creating a series of OTFTs with various channel dimensions.

The most stable pentacene **4** has limited solubility in organic solvents, while **2** could not form continuous thin films by solution deposition; thus, no satisfactory solution-processed OTFT devices could be fabricated. On the other hand, soluble pentacene **1** displayed insignificant FET activities when used as a solution-processed thin-film semiconductor. This was mostly likely due to the formation of spherulite crystalline structures in the channel semiconductor, which confined charge carriers within the spherulite aggregates and adversely hampered charge carrier transport across the semiconductor channel. This is in sharp contrast to the efficient charge carrier transport by rod-like crystal domains often observed in organic semiconductors where arrays of parallel semiconductor π -stacks were dominant.¹⁰ With pentacene **3**, the spin-coated thin-film semiconductor exhibited typical FET characteristics, affording a mobility of $\sim 0.01 \text{ cm}^2 \text{ V}^{-1} \text{ s}^{-1}$. Further improvement in mobility to $0.08 \text{ cm}^2 \text{ V}^{-1} \text{ s}^{-1}$ was achieved with a dip-coated thin-film semiconductor of **3** (Figure 5). The observed differences in FET mobility of semiconductor **3** fabricated by these two different solution deposition techniques suggested that slow solvent evaporation would be needed to permit establishment of higher molecular orders for efficient charge carrier transport. Accordingly, **3** was drop-cast from a dilute chlorobenzene solution and allowed to evaporate slowly in air, resulting in the formation of millimeter-sized ribbon-like single-crystals on the wafer surface. The gold source/drain electrode pairs were then deposited on top of the crystals to form a series of solution-processed, single-crystal OTFTs of different dimensions (Figure 6). These devices exhibited good saturation behaviors, near-zero turn-on voltage with no observable contact resistance. A FET mobility of $0.52 \text{ cm}^2 \text{ V}^{-1} \text{ s}^{-1}$ and current on/off ratio of 10^5 were obtained. Because the width of the crystal was too small to permit proper mounting of source/drain electrodes, the charge transport properties along the direction of the crystal width

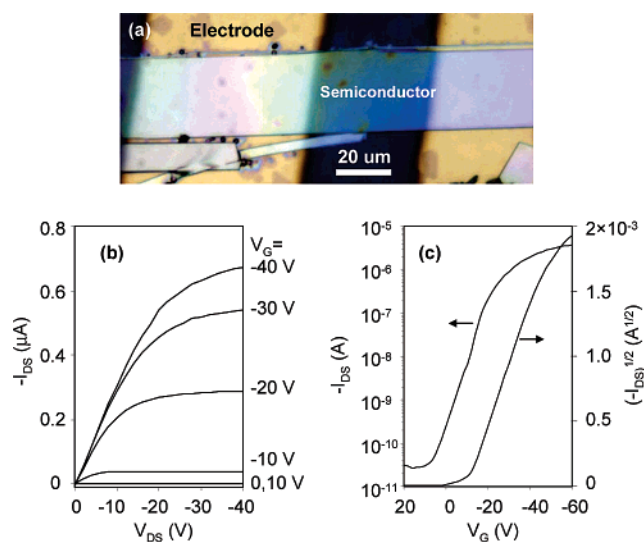


Figure 6. (a) Illustrative bottom-gate, top-contact OTFT using 6,13-bis(4-pentylphenyl-ethynyl)pentacene **3** as a semiconductor (channel length = $45 \mu\text{m}$ and channel width = $30 \mu\text{m}$); (b) its output curve; and (c) transfer curve at $V_{DS} = -60 \text{ V}$.

could not therefore be studied. For comparison, drop-cast single-crystal OTFTs using TIPS-pentacene **5** synthesized in our laboratory were also fabricated under the same experimental conditions. The highest mobility that we obtained with these devices was $\sim 0.42 \text{ cm}^2 \text{ V}^{-1} \text{ s}^{-1}$ (on/off ratio of 10^5), which is slightly lower than that of **3** under similar conditions. Accordingly, while it was believed that a parallel π -stacking arrayed structure is preferred in pentacene semiconductors for achieving high mobility,^{7c} our results clearly showed that a herringbone structural arrangement in a semiconductor such as that of **3** was as equally efficient, if not better for OTFTs, provided that appropriate functional groups are anchored to the pentacene nucleus. These are exciting results as photochemically stable pentacene derivatives that can serve as solution-processed, high-mobility semiconductors in OTFTs are generally very rare. Work is in progress to create large and continuous crystalline thin films of **3** to enable fabrication of OTFTs for large-area devices.

Conclusion

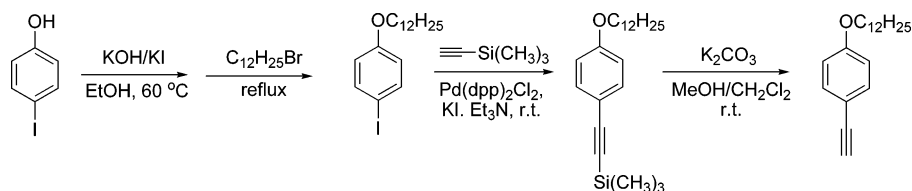
In conclusion, we have demonstrated that the photooxidative stability of a pentacene structure can be dramatically improved through appropriate substitution at its C-6/C-13 positions to promote extended π -electron delocalization via resonance/inductive effects. From the photooxidative stability, solution processability, and FET performance perspectives, an effective substituent is 4-alkylphenylethynyl, which enables achievement of excellent photooxidative stability as well as high FET mobility in a solution-processed thin-film semiconductor for OTFTs.

Experimental Procedures

Measurements. NMR spectra were recorded at room temperature on a Bruker DPX 300 NMR spectrometer in CDCl_3 with tetramethylsilane as an internal reference (0 ppm). UV-vis absorption spectra were obtained on a Varian Cary 5 UV-vis NIR spectro-

(10) (a) Ong, B. S.; Wu, Y.; Liu, P.; Gardner, S. *J. Am. Chem. Soc.* **2004**, *126*, 3378–3379. (b) Zhao, N.; Botton, G.; Zhu, S.; Duft, A.; Ong, B.; Wu, Y.; Liu, P. *Macromolecules* **2004**, *37*, 8307–8312.

Scheme 2. Synthesis of 1-Dodecyloxy-4-ethynylbenzene



photometer. IR spectra were obtained on a Nicolet Magna-IR 500 Series II spectrophotometer. Melting points were measured on TA Instruments DSC 2910 differential scanning calorimeter (DSC) at a heating rate of 5 °C per min under nitrogen atmosphere. Single-crystal X-ray diffraction was acquired on a Bruker Smart 6000 Cu CCD/RA diffractometer at room temperature.

Synthesis. All raw materials and solvents were purchased from Sigma-Aldrich and used as received without further purification. 6,13-Bis(triisopropylsilylethynyl)pentacene (TIPS-pentacene) **5** was synthesized according to literature methods.^{7a,11}

Synthesis of 1-Dodecyloxy-4-ethynylbenzene. 1-Dodecyloxy-4-ethynylbenzene was synthesized according to Scheme 2.

(a) *1-Dodecyl-4-iodobenzene.* To a well-stirred solution of 4-iodophenol (8.80 g, 40 mmol) in ethanol (100 mL) were added potassium hydroxide (2.24 g, 40 mmol) and potassium iodide (0.13 g, 2 mol %), and the mixture was heated to 60 °C. After the addition of 1-bromododecane in a dropwise fashion, the reaction mixture was refluxed for 12 h. After cooling to room temperature, the precipitate was filtered and purified by column chromatography on silica gel using methylene chloride/hexane (2:1, v/v) as the eluent. Yield: 11.47 g (73.9%).

¹H NMR: δ 7.38 (d, J = 9.1 Hz, 2H), 6.67 (d, J = 9.1 Hz, 2H), 3.91 (t, J = 6.6 Hz, 2H), 1.76 (m, 2H), 1.43 (m, 2H), 1.27 (m, 16H), 0.88 (t, J = 6.6 Hz, 3H).

(b) *1-Dodecyloxy-4-(trimethylsilyl)benzene.* To a solution of 1-dodecyl-4-iodobenzene (11.21 g, 28.87 mmol) and (trimethylsilyl)acetylene (3.40 g, 34.64 mmol) in triethylamine (200 mL) were added dichlorobis(triphenylphosphine)palladium (II) (0.41 g, 0.58 mmol) and copper(I) iodide (55 mg, 0.29 mmol) at 0 °C. The reaction mixture was stirred at 0 °C for 1 h and then at room temperature for 20 h under argon. After evaporation of the solvent, the crude product was purified by column chromatography on silica gel using ethyl acetate/hexane (1:9, v/v) as the eluent. Yield: 8.89 g (85.9%). ¹H NMR: δ 7.54 (d, J = 8.8 Hz, 2H), 6.80 (d, J = 8.8 Hz, 2H), 3.94 (t, J = 6.6 Hz, 2H), 1.77 (m, 2H), 1.44 (m, 2H), 1.26 (m, 16H), 0.88 (t, J = 6.9 Hz, 3H), 0.23 (s, 9H).

(c) *1-Dodecyloxy-4-ethynylbenzene.* To a solution of 1-dodecyl-4-(trimethylsilylethynyl)benzene (8.89 g, 24.8 mmol) in a mixture of methanol/methylene chloride (50 mL/50 mL) was added potassium carbonate (0.343 g, 2.48 mmol), and the mixture was stirred for 4 h at room temperature. After evaporation of solvent, the crude product was purified by column chromatography on silica gel using methylene chloride/hexane (1:4, v/v) as an eluent. Yield: 6.06 g (85.4%). ¹H NMR: δ 7.41 (d, J = 8.6 Hz, 2H), 6.83 (d, J = 8.6 Hz, 2H), 3.95 (t, J = 6.6 Hz, 2H), 2.99 (s, 1H), 1.78 (m, 2H), 1.44 (m, 2H), 1.26 (m, 16H), 0.88 (t, J = 6.8 Hz, 3H).

Synthesis of 6,13-Disubstituted Pentacenes. 6,13-Disubstituted pentacenes were synthesized according Scheme 1. The synthesis of **3** serves as an illustrative example. Compounds **1**, **2**, and **4** were synthesized in a similar manner.

(a) *6,13-Bis(4-pentylphenylethynyl)pentacene (3).* To isopropylmagnesium chloride (7.5 mL, 15 mmol, 2 M in THF) was added 1-ethynyl-4-pentylbenzene (2.58 g, 2.92 mL, 15 mmol) and 20 mL of THF. The mixture was heated at 60 °C for 30 min and then

cooled to room temperature. 6,13-Pentacenequinone (1 g, 3.24 mmol) was added, and the mixture was heated at 60 °C for 2 h until all solid disappeared and solution became dark brown. After cooling, a mixture of SnCl₂ (4 g, 21 mmol) in 10% HCl (10 mL) was added carefully until no bubbles appeared. The mixture was heated at 60 °C for additional 30 min and then cooled to room temperature and poured rapidly into 400 mL of methanol. The precipitated deep blue solid was filtered, washed with methanol, and dried. It was then dissolved in toluene (100 mL) and passed through a short silica gel column chromatography and recrystallized 5 times from hexane/toluene (1:2, v/v) (30 mL each to give pure 6,13-bis(4-pentylphenylethynyl)pentacene as a deep blue solid. Yield, 1.80 g (90%). ¹H NMR: δ 9.25 (s, 4H), 8.03 (dd, J_1 = 6.6 Hz, J_2 = 3.2 Hz, 4H), 7.82 (d, J = 8.1 Hz, 4H), 7.41 (dd, J_1 = 6.6 Hz, J_2 = 3.2 Hz, 4H), 7.35 (d, J = 8.1 Hz, 4H), 2.73 (t, J = 7.8 Hz, 4H), 1.72 (m, 4H), 1.37 – 1.42 (m, 8H), 0.95 (t, J = 7.0 Hz, 6H). ¹³C NMR: δ 143.94, 132.00, 131.71, 129.95, 128.74, 128.66, 125.97, 125.72, 120.94, 117.83, 104.61, 87.50, 36.05, 31.53, 31.07, 22.60, 14.09. UV-vis (toluene): 660, 607, 564 nm. IR (KBr): 3041, 2951, 2923, 2851, 1510, 1176, 946, 870, 839, 816, 738 cm⁻¹. Mp: 191 °C (dec).

(b) *6,13-Bis(dodecylethynyl)pentacene (1).* Yield: 75%. ¹H NMR: δ 9.19 (s, 4H), 8.01 (dd, J_1 = 6.6 Hz, J_2 = 3.2 Hz, 4H), 7.38 (dd, J_1 = 6.6 Hz, J_2 = 3.2 Hz, 4H), 2.94 (t, J = 7.0 Hz, 4H), 1.95 (m, 4H), 1.76 (m, 4H), 1.36 – 1.49 (m, 16H), 0.90 (t, J = 7.0 Hz, 6H). ¹³C NMR: δ 131.98, 130.40, 128.63, 126.05, 125.61, 118.21, 105.51, 78.86, 31.95, 29.44, 29.36, 29.18, 22.73, 20.64, 14.12. UV-vis (toluene): 625, 577, 539 nm. IR (KBr): 3049, 2951, 2923, 2853, 1465, 1387, 876, 740 cm⁻¹. Mp: 92 °C, 109 °C (dec).

(c) *6,13-Bis(4-dodecyloxyphenylethynyl)pentacene (2).* Yield: 55%. ¹H NMR: δ 9.24 (s, 4H), 8.03 (dd, J_1 = 6.9 Hz, J_2 = 3.0 Hz, 4H), 7.83 (d, J = 8.6 Hz, 4H), 7.41 (dd, J_1 = 6.9 Hz, J_2 = 3.0 Hz, 4H), 7.35 (d, J = 8.6 Hz, 4H), 4.08 (t, J = 6.6 Hz, 4H), 1.87 (m, 4H), 1.52 (m, 4H), 1.29–1.37 (m, 34H), 0.90 (t, J = 6.7 Hz, 6H). UV-vis (toluene): 664, 611, 566 nm. Mp: 162 °C (dec).

(d) *6,13-Bis(4-trifluoromethylphenyl)pentacene (4).* Yield: 64%. UV-vis (toluene): 662, 608, 565 nm. Mp: 243 °C (dec).

OTFT Fabrication and Characterization. Bottom-gate, top-contact OTFTs using these pentacene derivatives as channel semiconductors were fabricated under ambient conditions. A heavily doped silicon wafer was used as gate electrode, and its SiO₂ surface layer (~100 nm) as the gate dielectric. The SiO₂ surface was first cleaned with argon plasma, then washed with isopropanol, and air-dried. A 0.5 wt % solution of the pentacene derivative in chlorobenzene was used to form the semiconductor layer by spin-coating at 1000 rpm for 60 s or by dip-coating, followed by drying in a vacuum oven at 80 °C for about 1 h. Subsequently, gold source/drain electrode pairs were deposited by vacuum evaporation through a shadow mask, thus creating a series of OTFTs with various channel length (L) and width (W) dimensions. To prepare a single-crystal semiconductor on a wafer surface, a 0.05 wt % solution of compound **3** in chlorobenzene was used for casting. The wafer substrate was placed in a Petri dish. Several drops of the solution of **3** were placed on the wafer to cover its whole surface and allowed to evaporate slowly in air to dryness.

The OTFT devices were characterized in air using a Keithley 4200 semiconductor characterization system. The mobility in the saturated regimes was extracted from the following equation:

$$I_D = C_i \mu (W/2L)(V_G - V_T)^2$$

where W is the channel width, L is the channel length, I_D is the drain current, C_i is the capacitance per unit area of the gate dielectric layer, and V_G and V_T are, respectively, the gate voltage and threshold voltage. V_T of the device was determined from the relationship

between the square root of I_D at the saturated regime and V_G of the device by extrapolating the measured data to $I_D = 0$.

Acknowledgment. Partial financial support of this work is provided by the National Institute of Standards and Technology through an Advanced Technology Grant (70NANB0H3033).

Supporting Information Available: Single-crystal data for **3**. This material is available free of charge via the Internet at <http://pubs.acs.org>.

CM062378N